inside the boundary layer the direction of the normal velocity changes and the fluid moves away from the wall. This phenomenon is visible in Fig. 3, which shows a few streamlines. The viscous and thermal diffusion must be small for this phenomenon to appear. In other words the magnetic Prandtl number P_m must be lower than a critical value P_m^*. For an insulating wall this critical value falls in the interval (0.002, 0.005). For a cold wall it falls in the interval (0.03, 0.1) when $T_{(0)} = 1$. Both results are for the conditions $M_a = 3.323$, $M_v = 1$, $P_r = 1$.

In addition, the density shows a maximum in the middle of the boundary layer. This can be explained in the following way: As the fluid moves into the boundary layer it first undergoes an adiabatic compression under the influence of the magnetic pressure. (This can be seen by looking at the direction of the Lorentz force: $\boldsymbol{f} = \boldsymbol{j} \times \boldsymbol{b}$.) Thus, as the magnetic field decreases, the gas pressure rises. This adiabatic compression leads to an increase in the density, $\rho \sim p^{0.6}$, and in the temperature: $t \sim p^{0.4}$. As the gas penetrates inside the boundary layer the Ohmic heat release becomes significant and the compression is no longer isentropic. The temperature t increases under the influence of the Ohmic dissipation as well as the viscous friction. Since the pressure is approximately constant, the density decreases. Next to the wall the heat diffusion balances the heat generation (Ohmic and viscous friction), and the density may either increase or decrease depending on the type of boundary condition considered.

Experimental results that could be used to check the predictions of this analysis are difficult to find. The current distribution for the parallel-plate thruster tested by Di Capua and Jahn[6] is shown in Fig. 1, but other variables were not reported.

IV. Conclusions

It has been shown that the presence of insulating surfaces downstream of a plasma containing a residual magnetic field will give rise to very intense local heating along the surface of the insulator. This heating is the result of the recovery of the gas kinetic energy released by viscous friction, as well as the recovery of the residual electromagnetic energy released by Ohmic heating. At high values of the magnetic Reynolds number the flow is drawn towards the insulators and the density reaches a maximum in the middle of the boundary layer.

This article also proposes a new similarity method to solve boundary-layer problems. This method was applied to a compressible magnetodynamic boundary layer, but can also be applied to many boundary-layer problems traditionally studied using the Illingworth-Stewartson transformation.

References

[1]Wilcox, M. W., "The Magnetofluiddynamical Viscous Compressible Flow About Wedges and Flat Plates," *Proceedings of the 4th Biennial Gas Dynamics Symposium*, edited by A. B. Cambel, T. P. Anderson, and M. M. Slawsky, Northwestern Univ. Press, Evanston, IL, 1962, pp. 277–298.

[2]Fay, J. A., "Plasma Boundary Layers," *Proceedings of the 4th Biennial Gas Dynamics Symposium*, edited by A. B. Cambel, T. P. Anderson, and M. M. Slawsky, Northwestern Univ. Press, Evanston, IL, 1962, pp. 337–348.

[3]Moffat, W. C., "Approximate Solutions for the Skin Friction and Heat Transfer in MHD Channel Flows," Project Squid Technical Rept., MIT-36-P, Cambridge, MA, June 1965.

[4]Daily, J. W., Kruger, C. H., Self, S. A., and Eustis, R. H., "Boundary Layer Profile Measurements in a Combustion Driven MHD Generator," *6th International Conference on Magnetohydrodynamic Electrical Power Generation*, Vol. 1 (Washington, DC), National Technical Information Services, Springfield, VA, 1975, pp. 451–463.

[5]Pai, S. I., *Magnetogasdynamics and Plasma Dynamics*, Springer-Verlag, Vienna, Austria, 1963, pp. 67, 68.

[6]Di Capua, M. S., and Jahn, R. G., "Energy Deposition in Parallel-Plate Plasma Accelerators," AIAA Paper 71-197, Jan. 1971.

[7]Ascher, U. M., Mattheij, R. M. M., and Russel, R. D., *Numerical Solution of Boundary Value Problems for Ordinary Differential Equations*, Prentice Hall, Englewood Cliffs, NJ, 1988, pp. 526–533.

Unsteady Heat Transfer from a Thick Hot-Film Sensor

Chong H. Park* and Kevin D. Cole†
University of Nebraska at Lincoln, Lincoln, Nebraska 68588

Introduction

METAL-FILM sensors have been widely used as temperature sensors, heat flux sensors, shear-stress sensors, and recently as separation detectors. In all of these applications, the thermal storage in the sensor can be neglected if the metal film is "thin." Schultz and Jones[1] indicate that the thermal storage in the sensor may be neglected for heat flux sensors in a flow containing frequencies below 10 kHz if the metal film is less than 0.1 μm. However, the sensor studied in this Note has a thick metal film with thickness e of 6 μm on a polymer substrate that is glued to a surface for use in an airflow. The advantage of a thick-metal sensor is that it can carry more electric current, and therefore gives a higher output voltage. The present research is to develop numerical and analytical models of the thick sensor that include thermal storage in the sensor.

Transient conjugate heat transfer analysis is carried out with the unsteady surface element (USE) method. The USE method is a boundary discretization method and is a very efficient method for solving conjugate heat transfer problems.[2] In this Note, the temperature response of the sensor is determined from analysis of three bodies (air, hot film, and polymer substrate). The average temperature of the hot-film sensor is determined, with known heat flux input to the hot film and with known air velocity. The present work that involves steady airflow with transient heat transfer is a first step toward transient airflow analysis of these sensors.

Boundary Value Problem

Figure 1 shows the geometry of the conjugate heat transfer problem. The two-dimensional geometry applied here is appropriate for the large aspect ratio ($b/a = 85$) hot-film sensor. Refer to Park and Cole[3] for the actual configuration for hot-film sensors provided by Pratt & Whitney United Technologies. The parameters a and b are streamwise and spanwise half-length of the hot film, respectively. All material properties are treated as constant values (small temperature rise assumed). A single-layer substrate with an effective thickness D is used to represent the actual multiple-layered solid composed of a polymer layer, glue layer, and the underlying metal surface to which the sensor is glued. For airflow, radiation and natural convection are neglected, viscous dissipation is neglected, and the streamwise conduction in the flow is neglected. The airflow has a linear velocity profile ($u = \beta y_f$). Although the hot film is thermally thick, it is mechanically so small that it does not disturb the airflow.

Received Oct. 25, 1993; revision received Feb. 22, 1994; accepted for publication Feb. 25, 1994.

*Instructor, Mechanical Engineering Department.

†Associate Professor, Mechanical Engineering Department. Member AIAA.

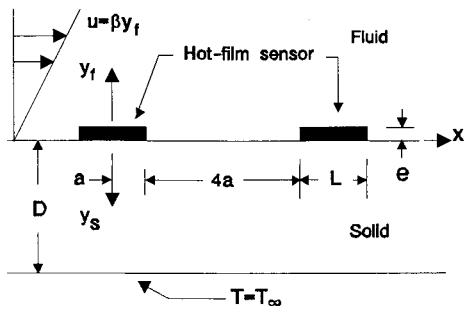

Fig. 1 Geometry for conjugate heat transfer.

The energy equations of this problem are different for each region:

Fluid

$$\beta y_f \frac{\partial T_f}{\partial x} = \alpha_f \frac{\partial^2 T_f}{\partial (y_f)^2}; \quad 0 < y_f < \infty, \quad -\infty < x < +\infty \tag{1}$$

Substrate

$$\frac{1}{\alpha_s}\frac{\partial T_s}{\partial t} = \frac{\partial^2 T_s}{\partial x^2} + \frac{\partial^2 T_s}{\partial (y_s)^2}; \quad 0 < y_s < D, \quad -\infty < x < +\infty \tag{2}$$

Hot film

$$\frac{1}{\alpha_h}\frac{\partial T_h}{\partial t} = \frac{\partial^2 T_h}{\partial x^2} - m^2(x, t)(T_h - T_\infty) + \frac{g(t)}{k_h}$$
$$0 < y_h < e, \quad -a < x < +a, \quad 5a < x < 7a \tag{3}$$

where $m^2(x, t) = (1/k_h e)\cdot[(q_f + q_s)/T_h]$, $q_f(x, y_f, t) = -k_f(\partial T_f/\partial y_f)$, and $q_s(x, y_s, t) = -k_s(\partial T_s/\partial y_s)$. The parameters T and q represent temperature and heat flux. The parameters x and y are streamwise coordinate and coordinate normal to the interface. The parameters k, α, and β are thermal conductivity, thermal diffusivity, and fluid velocity gradient, respectively. Parameter g represents volumetric heat generation in the hot film that produces all of the heat transfer. The subscripts f, s, and h indicate fluid, substrate, and hot film, respectively. The first term in Eq. (3) represents the heat storage in the hot film.

The initial temperature distribution $T(x, y, t = 0)$ is equal to the ambient temperature T_∞. Perfect thermal contact exists at the interfaces between the fluid, the surface of the substrate, and the hot film. The boundary conditions of the entire domain are given by

$$T_f(x \to \pm\infty, y_f, t) - T_\infty = T_s(x \to \pm\infty, y_s, t) - T_\infty = 0 \tag{4}$$

$$T_f(x, y_f \to \infty, t) - T_\infty = T_s(x, y_s \to D, t) - T_\infty = 0 \tag{5}$$

Solution Method

The temperature in the three-body system can be determined with the USE method. The method involves matching the temperature at discrete surface elements on the active interfaces between the air, hot film, and substrate. The heat flux is assumed to be piecewise constant over each surface element. The temperature expression for each body has the form

$$T(x, y = 0, t) = \sum_{j=1}^{N} \int_{\lambda=0}^{t} q(x_j', \lambda)\phi(x - x', t - \lambda)\, d\lambda \tag{6}$$

where q is the unknown heat flux history on the j surface element, and ϕ is a known influence function (Park,[4] Chap. 2). The three integral expressions are solved numerically for the unknown heat flux histories and for the unknown temperature distribution on the hot film.

An analytical solution is possible at "early time." Initially, the sensor is "cold," at ambient temperature, and at $t = 0$ the heating begins. Soon after the constant-current circuit is turned on, heat is stored in the hot film itself, and heat also flows from the hot film normal to the interface. In this early time period, the metal film and the substrate dominate the heat transfer so that convection can be neglected. Under the restriction of early time, all fluid terms in Eq. (3) are neglected, the term $\partial^2 T/\partial x^2$ in Eq. (3) is also neglected, and then the solution is given by Park[3]

$$T_{av}^{+} = \frac{T_{av}(t) - T_\infty}{q_0 a/k_s} = 2B\sqrt{(t^+/\pi)} - Ct^+ + (B/A)\cdot[\exp(A^2 t^+)\operatorname{erfc}(A\sqrt{t^+}) - 1] \tag{7}$$

where

$$A = \frac{(\rho c a)_s}{(\rho c e_h)} - \frac{1}{\pi}$$
$$B = 1 + \frac{2}{\pi A} + \frac{1}{\pi^2 A^2} \tag{8}$$
$$C = \frac{1}{\pi} + \frac{1}{\pi^2 A}$$

The parameter q_0 is the total heat flux supplied to the sensor. Cole and Beck[2] limited this type of analytical solution to the dimensionless time, $0 < t^+ < 0.3$, where $t^+ = \alpha_s t/a^2$.

Results

The results for the spatial average temperature on the sensor are presented in Table 1 in dimensionless form. The thermal diffusivity of the substrate α_s is 1.0×10^{-7} m²/s. The ratio $(\rho ca)_s/(\rho ce)_h$ is a dimensionless parameter that describes the effect of the hot film thickness on the transient temperature $[(\rho c)_s/(\rho c)_h = 0.395]$. At a very early time, the numerical method agrees well with the approximate analytical solution for the spatial average temperature of the thick sensor ($e = 6 \times 10^{-6}$ m). This analytical solution is a valuable tool that serves as a check on the numerical method in this time range.

The dimensionless spatial average temperature of the sensor is plotted vs dimensionless time with several values of hot-film thickness in Fig. 2. The heat storage in the metal sensor occurs in a very short time because of the high thermal conductivity of the metal compared to the polymer substrate (26 W/m K metal; 0.1542 W/m K polymer). If the sensor thickness becomes small ($e \to 0$), its transient temperature distribution becomes identical to the result given by Cole and Beck.[2] The thin sensor ($e = 0$) spatial average temperature rises much faster than the thick sensor temperature because of thermal storage in the thick sensor. All four curves reach 95% of the steady-state temperature at the dimensionless time $t^+ \approx 20$ ($t \approx 0.025$ s, $\alpha_s = 1.0 \times 10^{-7}$ m²/s, and $a = 11.25$ μm).

Table 1 Early-time T_{av}^{+} results for β = 10,340/s, e/a = 0.531, and D/a = 4

Time t^+	Analytical solution	Numerical solution	Percent difference
0.0003	0.220884*E*-3	0.220793*E*-3	0.041
0.0008	0.585418*E*-3	0.585359*E*-3	0.010
0.0030	0.216296*E*-2	0.216074*E*-2	0.103
0.0070	0.496567*E*-2	0.496554*E*-2	0.003
0.0300	0.202341*E*-1	0.201679*E*-1	0.327
0.0700	0.448288*E*-1	0.447705*E*-1	0.130
0.1000	0.621826*E*-1	0.621113*E*-1	0.115

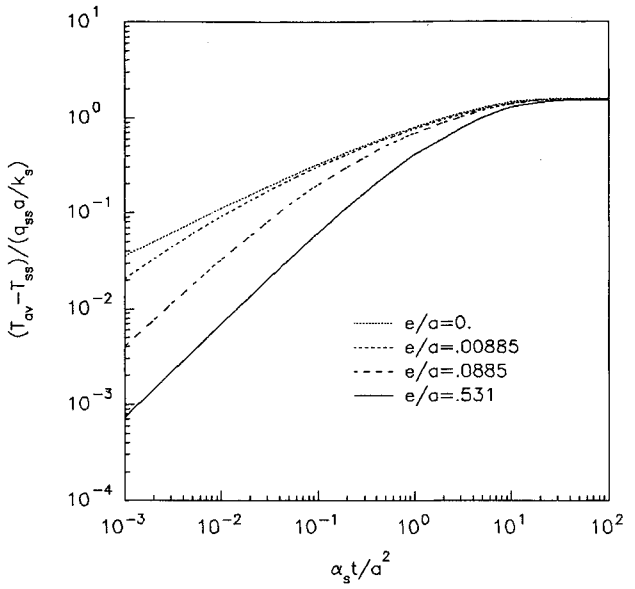

Fig. 2 Spatial average temperature of the sensor vs time for several values of hot-film thickness obtained from the USE simulation (β = 10,340/s, D/a = 4).

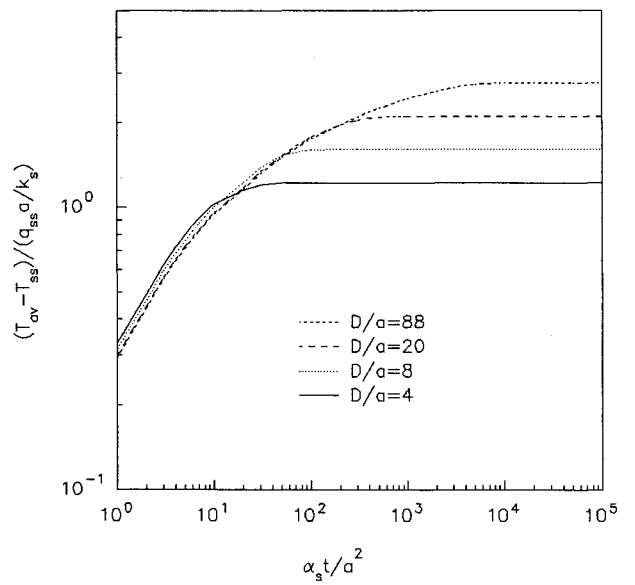

Fig. 3 Spatial average temperature of the sensor vs time for several values of substrate thickness obtained from the USE simulation (β = 10,340/s, e/a = 0.531).

Therefore, thermal storage in the hot-film sensor can be neglected for a thermal transient containing frequencies below approximately 40 Hz (corresponding to $t \approx 0.025$ s).

Figure 3 is a log-log plot of the spatial average temperature of the sensor vs time for several values of substrate thickness D/a. The numerical solution includes the heat loss through the electric leads. The ratio of the total heat lost to the electric leads to the total introduced heat, Q_l/Q_0 has the following values: 0.1977 (D/a = 4); 0.2390 (D/a = 8); 0.2748 (D/a = 20); 0.2910 (D/a = 88). The shift of each plot at small times, before steady state is reached, is caused by the different values of Q_l/Q_0. If the influence of Q_l were not included, Fig. 3 would be similar to the work done by Cole and Beck.[2] The D/a = 4 (thin substrate) case reaches steady state first with the lowest average temperature. The thicker substrate cases reach steady state at successively later times, each with a successively higher average temperature. The time to steady state can be estimated approximately by D^2/α_s, or by $t^+ = (D/a)^2$, since the heat transfer to the substrate dominates the time to reach steady state.

The transient computations were performed on a VAX 8800 computer using up to 35 surface elements in the substrate (14 on the hot-film) and an active interface of length of up to 281 times the hot-film size. Computation time for one run of the transient calculation was about 180 CPU s.

Conclusions

The constant-current responses of a thick hot-film sensor in steady airflow were computed by the USE method. Numerical results are in good agreement with the analytical solution for the spatial average temperature of the sensor at very early time. The heat storage in the metal sensor is important only at the beginning of the step response corresponding to higher frequency transients. Thus, the thermal storage in the thick hot-film sensor (e = 6 μm) may be neglected for a thermal transient containing frequencies approximately below 40 Hz. The time to steady state is controlled by the value of D, the effective substrate thickness, and not by the sensor thickness e, since the overall thermal mass is dominated by the substrate. Future research will include the analysis of airflow with an oscillating component.

References

[1]Schultz, D. L., and Jones, T. V., "Heat Transfer Research in Short Duration Hypersonic Facilities," AGARD AG-165, 1973.

[2]Cole, K. D., and Beck, J. V., "Conjugated Heat Transfer from a Strip Heater with the Unsteady Surface Element Method," *Journal of Thermophysics and Heat Transfer*, Vol. 1, No. 4, 1987, pp. 348–354.

[3]Park, C. H., and Cole, K. D., "Theory and Experiment for Metal-on-Polymer Shear Stress Sensor in Air Flow," *Proceedings of the American Society of Mechanical Engineering National Heat Transfer Conference* (Atlanta, GA), HTD-Vol. 249, 1993, pp. 61–71.

[4]Park, C. H., "Shear Stress Measurements with Metal-on-Polymer Shear Stress Sensor-Analysis and Experiment," Ph.D. Dissertation, Univ. of Nebraska, Lincoln, NE, 1994, pp. 71–78.

Unsteady Heat Transfer from a Sphere at Low Reynolds and Strouhal Numbers

Y. Bayazitoglu,* C. F. Anderson,† R. D. Cohen,‡ and R. W. Shampine†
Rice University, Houston, Texas 77251

Nomenclature

A_p = surface area of particle
D = particle diameter
k = thermal conductivity of the fluid
Nu_0 = steady Nusselt number at the acoustic Reynolds number

Presented as Paper 93-0915 at the AIAA 31st Aerospace Sciences Meeting, Reno, NV, Jan. 11–14, 1993; received Aug. 12, 1993; revision received Jan. 24, 1994; accepted for publication Jan. 26, 1994.

*Professor, Department of Mechanical Engineering and Materials Science, P.O. Box 1892. Member AIAA.

†Graduate Student, Department of Mechanical Engineering and Materials Science, P.O. Box 1892.

‡Associate Professor, Department of Mechanical Engineering and Materials Science, P.O. Box 1892.